Computational study of organized cycloaddition reactions with pyrrole moiety as a diene

Branko S. Jursic

Department of Chemistry, University of New Orleans, New Orleans, Louisiana 70148, USA

Received (in Gainesville, FL) 18th May 1998, Accepted 14th October 1998

Computational studies were performed to determine the reactivity of pyrrole as the diene in cycloaddition reactions, and to investigate the necessary chemical transformations that would make pyrrole an effective diene. Also, it was of interest to establish what chemical transformations would lead exclusively to an *exo* or to *endo* cycloadducts. The study was performed by using the pyrrole ring bond order uniformity, transition state six-membered ring bond order uniformity, frontier molecular orbital energy changes (inertia principle), and activation energies. Synthetic routes for the preparation of one isomer over another were proposed.

Introduction

One of the most widely used reactions in multiple step syntheses[1] of natural products is the Diels–Alder reaction.[2] One major source of dienophiles for the Diels–Alder reaction are the aromatic five-membered ring heterocyclic compounds.[3] However, they are not the most reactive dienophiles due to their high aromaticity (double bond delocalization). The primary goal in making them more reactive is to localize double and single bonds in the ring through decreasing the heteroatom lone pair contribution in the ring orbital overlap. For instance, we have demonstrated that oxidation of thiophene sulfur drastically increases its reactivity as diene in the Diels–Alder reaction.[4] This was later confirmed by preparing several cycloadducts with oxidized thiophene.[5] Similar predictions were made for protonated pyrroles,[6] however, it is well known that the pyrrole ring is not easily protonated. Pyrrole is a particularly good starting material for the preparation of natural product derivatives, such as the analogs of alkaloids.[7] In the majority of the reactions with pyrrole as a dimer, an *endo* cycloadduct is the dominant product; although for the preparation of alkaloids, an *exo* cycloadduct is desirable. Here, we present our computational study of the cycloaddition reaction with pyrrole derivatives, which leads exclusively to *exo* cycloadducts.

Computational methodology

All computational studies were performed with the AM1[8] semiempirical method as a part of the MOPAC[9] computational package. Bond orders were computed with the AM1 method as incorporated in the MOPAC computational package.[10] The density functional theory computational study was performed with the hybrid B3LYP[11] method with a 6-31G(d,p)[12] basis set as a part of the GAUSSIAN94[13] computational package.

Results and discussion

As mentioned above, the major reason why five-membered ring heterocycles are not efficient dienes in the Diels–Alder reaction is due to a high aromatic stabilization[14] that includes p-orbital overlap with the heteroatom lone electron pair. Recently, we have explored the aromaticity of five-membered ring heterocycles through their computed magnetic properties, as well as through their ring bond order uniformity.[15] We have also demonstrated that if a chemical transformation on the heterocycle is performed in such a way that the double and single bonds are more localized in the heterocyclic ring, then the heterocycle becomes more reactive.[16] Here, we will again demonstrate the usefulness of this approach in determining reactivities of pyrrole and its derivatives as the dienes for the Diels–Alder reaction.

The AM1 computed ring bond orders for pyrrole and its derivatives are presented in Table 1.[17] According to this approach, the more uniform the bond order in unsaturated heterocycles, the more aromatic the heterocycle (and consequently, less reactive). The measure of the bond order uniformity is through the summation of the ring bond orders, derived from averaging the ring bond order (SBOD). The smaller the bond order deviation, the less reactive the aromatic ring is in the Diels–Alder cycloaddition. SBOD in pyrrole is only 0.814, which makes pyrrole a very poor diene for cycloaddition reactions. The derivatization of pyrrole using SBOD increases its reactivity. For instance, in *N*-formylpyrrole the SBOD is higher, indicating higher localization of the CC double bond and consequently, a higher reactivity in the cycloaddition reaction is seen. This is due to the partial delocalization of the nitrogen lone electron pair on the amide oxygen, thus making the pyrrole ring less aromatic. The most pronounced localization of the single and double CC bonds in the pyrrole ring was obtained in *N*-methylpyrrolium cation. The nitrogen lone pair is now localized in the sigma NC bond with the methyl group and the *N*-methylpyrrolium cation becomes a highly reactive diene (Table 1).

Let us now explore the reactivity of these dienes in the cycloaddition reactions with 1,3-dioxacyclopent-4-ene, maleimide, and *N*-methylmaleimide. The AM1 computed transition structures for an *endo* addition are presented in Fig. 1. All transition states are for concerted formation of both CC bonds. When both diene and dienophile are symmetrical the transition state for synchronous bond formation can be computed. All bonds in this case are slightly longer than 2 Å (Fig. 1). Similar transition state structures are obtained for an *exo* cycloaddition.

If we consider the ground-state benzene molecule in terms of an interaction molecular orbital diagram, then six p-orbitals are arranged on a ring, each interacting with its neighbors. The transition state diagram for the Diels–Alder (p2s + p4s cycloaddition) reaction is identical. Therefore, the transition state will prefer the same stabilization as the benzene ground

Table 1 The bond order uniformity for pyrrole and its derivatives[a]

Heterocycle	BO_{12}	BO_{23}	BO_{34}	BO_{45}	BO_{51}	ABO	SBOD
Pyrrole	1.181	1.555	1.285	1.555	1.181	1.351	0.814
N-Methylpyrrole	1.160	1.557	1.280	1.557	1.160	1.343	0.857
N-Formylpyrrole	1.088	1.648	1.204	1.649	1.079	1.334	1.260
N-Methylpyrrolium	0.915	1.856	1.046	1.856	0.915	1.318	2.154

[a] BO_{nm} = bond order between the pyrrole ring atoms *n* and *m*; ABO = average ring bond order computed as sum of all ring bond orders divided by the number of atoms in the ring (five); SBOD = sum of ring bond order deviation from an average bond order.

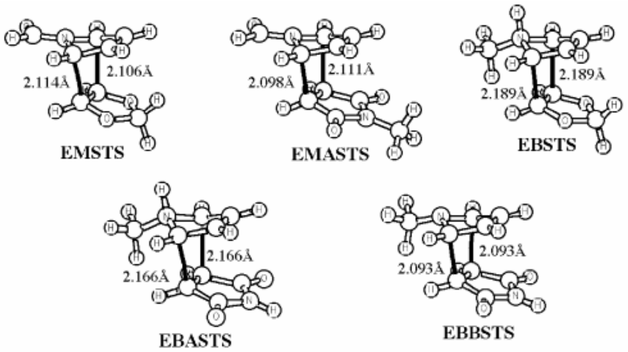

Fig. 1 The AM1 computed *endo* transition state structures for classical cycloaddition reaction with the pyrrole derivatives as dienes. Corresponding *exo* transition state structures are MSTS, MASTS, BSTS, BASTS and BBSTS respectively.

state. This analogy between benzene and the Diels–Alder transition state was first pointed out by Evans.[18] Later on, this principle was further developed by Zimmerman[19] and Dewar.[20] If we apply our bond order uniformity principle through some bond order deviations from an average bond order, then the most reactive reactant pair is the one that will form transition state structures with the highest bond order uniformity. The bond order deviation was computed from the six-membered transition state ring as shown in Table 2. It clearly demonstrates that the most uniform bond order distribution is for the *endo* transition state structures of the maleimide addition to *N*-methylpyrrolium cation (**EBASTS**). One can expect that this transition state should have a very low activation barrier. If we now consider the *exo–endo* cycloaddition reactions for the maleimide addition to *N*-methylpyrrolium (**BASTS** and **EBASTS**) and *N*-methylpyrrole (**BBSTS** and **EBBSTS**), in both cases it becomes clear that the *endo* transition state structures have a slightly higher uniformity, which may suggest that the formation of an *endo* cycloadduct is preferable in comparison with the formation of its isomeric *exo* cycloadduct. This is well established in chemistry as the Alder *endo* rule.[21] Woodward and Hoffmann used secondary orbital interactions (SOI) between the diene and the dienophile to explain *endo* selectivity.[22] Bond orders in general can be used to determine reactivity,[23] as well as SOI in the transition state structures. We have used this approach to demonstrate SOI in the *endo* transition state for the cyclopropene addition to butadiene.[24] If stronger SOIs are possible in an *exo* transition state structure, then the *exo* cycloadduct is preferred over an *endo* cycloadduct.[25] In an attempt to demonstrate the influence of SOI on the reaction outcome, we can explore these interactions through bond orders in transition state structures in *exo* and *endo* transition state structures for the maleimide addition to *N*-methylpyrroles (transition state structures **BBSTS** and **EBBSTS** respectively). In the *endo* transition state structure **EBBSTS,** there are two bonds that form with identical bond orders 0.454. But, there are also orbital interactions between carbonyl carbons of the maleimide moiety of the transition state structure with molecular orbitals in C2, C3, C4 and C5 of the *N*-methylpyrrole moiety of the *endo* transition states. Due to the symmetric character of the transition state, bond orders are identical with respect to the C2 and C5 bond. The imide carbon bond orbital interactions with C2 and C3 atoms of the pyrrole moiety of the **EBBSTS** are 0.008434 and 0.002675, respectively. These values are relatively small but indicate substantial SOI in the *endo* transition state. Of course, for the *exo* transition states, these interactions are eliminated. If steric interactions between the diene and dienophile are substantial, then the formation of the *endo* transition is unfavorable and therefore SOI does not play an important role in the stabilization of the transition state structures. However, for many of the Diels–Alder reactions, they are of importance, and hence the formation of an *endo* cycloadduct is preferred.

One very useful approach in determining the qualitative reactivity of various dienophiles and dienes for the Diels–Alder reaction is through the evaluation of their frontier molecular orbital (FMO) energies. According to this approach[26] the reactant pair that shows the smallest difference between HOMO and LUMO orbitals should be the most reactive one. In this case the most reactive pair should be the 1,3-dioxacyclopent-4-ene and *N*-methylpyrrolium cation. The FMO energy difference is only 3.69 eV, while the least reactive is the maleimide addition to *N*-formylpyrrole with 8.96 eV (Table 3). In attempts to use the necessary frontier molecular orbital energy change (FMOC) to achieve transition state, FMO energies as a measure of reactivity evidently failed due to the fact that the starting energies for these reactions are substantially different. Thus, it appears that the list of reactivities (one that requires the major energy change) should actually be the most reactive reactants pair studied. A much more realistic picture can be obtained if only changes of molecular orbital energies for different pyrroles are considered in the reaction with the same dienophile, for instance, maleimide (Table 4). Considering the using of inertia,[27] which we have discussed previously, **the transition state that requires smaller** changes in the FMO energies, and bond order distribution is preferred. In our case, the most reactive cycloaddition reaction is with the *N*-methylpyrrolium cation, then with *N*-formylpyrrole, and finally with *N*-methylpyrrole (Table 4). All these reactions require frontier orbital changes in the pyrroles that are smaller for *endo* than for *exo* transition state structures, again confirming the validity of the Alder rule.

Let us now verify the qualitative study of the Diels–Alder cycloaddition reaction, with pyrrole as the diene, by computing activation barriers (Table 5). From computed activation barriers, it is obvious that the *endo* transition state structure is always preferred, as was demonstrated in the example of the inertia. The most reactive pair studied here is with *N*-methylpyrrolium cation as a pyrrole. Although the *endo* transition state structure has a lower energy, the *exo* cycloadduct is a more stable product. These observations are in full agreement with the vast knowledge of the Diels–Alder cycloaddition reactions previously studied. Therefore, preparation of an *exo* cycloadduct only as one of the intermediates in a synthesis of an alkaloid is not an easy task.

To overcome this problem we have devised special derivatives of pyrrole that contain a dienophile label attached to the pyrrole ring. There is some experimental evidence that suggests that intramolecular cycloaddition reactions with pyrroles are feasible.[28] The first group of such pyrrole derivatives is pre-

Table 2 Bond order uniformity for the six-membered ring transition states in the Diels–Alder reaction[a]

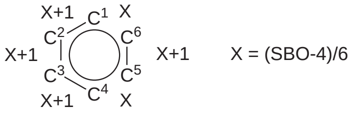

TS	BO_{12}	BO_{23}	BO_{34}	BO_{45}	BO_{56}	BO_{16}	X	SBOD
MSTS	1.213	1.609	1.217	0.437	1.318	0.449	0.374	0.747
EMSTS	1.221	1.605	1.219	0.451	1.312	0.447	0.376	0.751
MASTS	1.195	1.629	1.200	0.433	1.349	0.457	0.377	0.775
EMASTS	1.204	1.621	1.204	0.448	1.347	0.456	0.380	0.770
BSTS	1.400	1.421	1.400	0.362	1.364	0.362	0.385	0.133
EBSTS	1.395	1.419	1.395	0.359	1.353	0.359	0.380	0.138
BASTS	1.411	1.411	1.411	0.372	1.450	0.372	0.405	0.129
EBASTS	1.409	1.409	1.409	0.377	1.450	0.377	0.405	0.113
BBSTS	1.151	1.682	1.151	0.456	1.325	0.456	0.370	0.967
EBBSTS	1.176	1.653	1.176	0.454	1.337	0.454	0.375	0.872

[a] BO_{nm} = bond order between the pyrrole ring atoms *n* and *m*; ABO = average ring bond order computed as sum of all ring bond orders divided by number of atoms in the ring (five); SBOD = sum of ring bond order deviation from an average bond order.

Table 3 Frontier molecular orbital (FMO) energy (eV) changes for model *exo* and *endo* cycloaddition reactions

TS	$HOMO_R$	$LUMO_R$	$HOMO_{TS}$	$LUMO_{TS}$	ΔFMO	FMOC
MSTS	−9.00467	−0.03948[a]	−8.40826	0.14368	8.96519	0.77957
EMSTS	−9.00467	−0.03948[a]	−8.42619	0.10192	8.96519	0.71988
MASTS	−9.20382[a]	−1.14187	−9.65626	−0.71369	8.06195	0.88062
EMASTS	−9.20382[a]	−1.14187	−9.78774	−0.57645	8.06195	1.14934
BSTS	−9.00467	−5.30840[a]	−12.77582	−4.95381	3.69627	4.12574
EBSTS	−9.00467	−5.30840[a]	−12.62251	−4.85549	3.69627	4.07075
BASTS	−11.26571	−5.30840[a]	−14.16869	−5.50947	5.95731	3.10405
EBASTS	−11.26571	−5.30840[a]	−14.20684	−5.47179	5.95731	3.10452
BBSTS	−8.60554[a]	−1.21019	−9.41316	−0.44425	7.39535	1.57256
EBBSTS	−8.60554[a]	−1.21019	−9.53785	−0.31032	7.39535	1.83218

[a] Frontier molecular orbital energy for pyrrole derivative. Subscript R = reactant; subscript TS = transition state.

Table 4 Frontier molecular orbital (FMO) energy (eV) changes for both reactants to adapt the transition state energies

TS	$HOMO_P$	$LUMO_P$	$HOMO_{TS}$	$LUMO_{TS}$	OSFMOC
MASTSA	−9.20382	−0.03948	−9.73387	−0.76098	1.25155
EMASTSA	−9.20382	−0.03948	−9.85439	−0.62384	1.23493
BASTS	−14.89788	−5.30840	−14.16869	−5.50947	0.93026
EBASTS	−14.89788	−5.30840	−14.20684	−5.47179	0.85443
BBSTS	−8.60554	1.33135	−9.41316	−0.44425	2.58322
EBBSTS	−8.60554	1.33135	−9.53785	−0.31032	2.57398

HOMO energy for maleimide is −11.26571 eV; LUMO energy for maleimide is −1.21019 eV. Subscript P = product; subscript TS = transition state.

Table 5 Total energies (a.u.) for reactants and the transition state structures and activation barriers (kcal mol^{-1}) for template pyrrole cycloaddition reaction computed with B3LYP/6-31G(d)//AM1 theory model[a]

TS	E_R	E_{TS}	E_P	ΔE_I	ΔE_{II}
MSTS	−590.60302369	−590.5515102	−590.611725984	32.3	−5.5
EMSTS	−590.60302369	−590.5553102	−590.609060288	29.9	−3.8
MASTS	−722.23569676	−722.1939154	−722.239505071	26.2	−2.3
EMASTS	−722.23569676	−722.1945388	−722.235199368	25.8	0.3
BSTS	−516.90468738	−516.8687092	−516.959993926	22.6	−34.7
EBSTS	−516.90468738	−516.8803671	−516.955698242	15.3	−32.0
BASTS	−609.22328282	−609.1727780	−609.258079605	31.7	−21.8
EBASTS	−609.22328282	−609.1835169	−609.262546224	25.0	−24.4
BBSTS	−608.89958017	−608.8557353	−608.883726234	27.5	9.9
EBBSTS	−608.89958017	−608.8603075	−608.890539239	24.6	5.6

[a] E_R = total energy of the reactant; E_{TS} = total energy of the transition state; E_P = total energy of the product; ΔE_I = activation barrier (kcal mol^{-1}); ΔE_{II} = heat of the reaction (kcal mol^{-1}).

sented in Fig. 2. It is reasonable to expect that the pyrrole ring bond order uniformity would be similar to that obtained for their analogs without the dienophile moiety presented in Table 1. This assumption is valid (Table 6). The computed bond order uniformity for the pyrrole ring selects the pyrrolium cation derivatives **BR0** and **BAR0** as those with a higher localization of double bonds in the pyrrole ring; therefore, they should be very reactive. On the other hand, *N*-alkylated pyrrole in the reactant **BBR0** has the most uniform ring bond order distribution; hence, it should be the least reactive of all the pyrrole derivatives presented in Table 6.

It is conceivable that for a very short methylene linkage

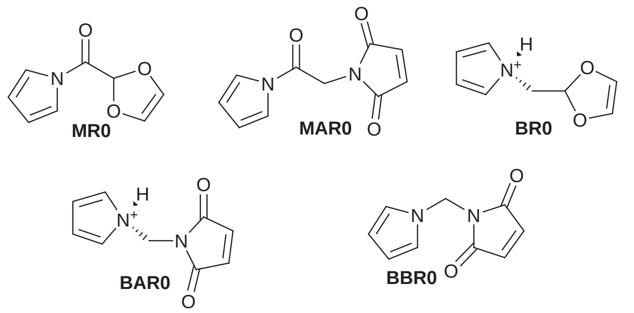

Fig. 2 Structures of first reactants in the studied series for intramolecular cycloaddition reaction.

Table 6 The heterocycle bond order uniformity in pyrrole ring of the first reactants presented in Fig. 2[a]

Reactant	BO_{12}	BO_{23}	BO_{34}	BO_{45}	BO_{51}	ABO	SBOD
MR0	1.079	1.651	1.201	1.651	1.081	1.333	1.274
MAR0	1.079	1.646	1.206	1.646	1.087	1.333	1.253
BR0	0.912	1.858	1.047	1.853	0.916	1.317	2.153
BAR0	0.922	1.852	1.049	1.852	0.922	1.319	2.130
BBR0	1.129	1.598	1.246	1.598	1.129	1.340	1.032

[a] BO_{nm} = bond order between the pyrrole ring atoms *n* and *m*; ABO = average ring bond order computed as sum of all rings bond orders divided by number of atoms in the ring (five); SBOD = sum of ring bond order deviation from an average bond order.

between diene and dienophile, the cycloaddition reaction is hampered due to the bond angle strain that should be present in the intramolecular cycloaddition reaction for the reactants presented in Fig. 2. Therefore, we have performed computational studies on such reactants that have various linkage sizes ($n = 0$–3, Fig. 3) hoping that with a certain distance between the diene and the dienophile, energy constraints will be eliminated, or at least become unimportant. The cartoons of these transition state structures are represented in Fig. 3, with the CC bond distance of new bonds being formed listed in Table 7. Again, all of these transition state structures are for the concerted mechanism of the cycloaddition reaction, and in some cases, they are for the synchronous formation of both CC bonds. For the majority of them, the bond distance is between 2.0 and 2.2 Å (Table 7), which is typical of the Diels–Alder transition state structures.[29] If we assume that the bond angle strains will be very small, or even present at all in the transition state where the diene and dienophile are separated by three methylene groups ($n = 2$, Fig. 3), then they represent the best choice for the evaluation of the six-membered transition state ring bond order uniformity. The AM1 computed values are presented in Table 8. As expected from the results presented above, the six-membered transition state structure for the protonated pyrrole derivative has the highest bond order uniformity, and therefore is more aromatic than, for instance, the transition state ring with *N*-alkylpyrrole (Table 8). As also mentioned above, we have to be cautious when the relative reactivity on the basis of the transition state ring's bond order uniformity is considered. If we were to compare the relative reactivity of these compounds, it is actually better to compare the changes of bond order uniformity going from the reaction to the transition state structure for the pyrrole ring. In this case, **BTS2** should be the most reactive and **BATS2** should be the least reactive. To confirm this finding, activation barriers for the intramolecular cycloaddition reaction with pyrrole as the dienophile were computed (Table 9). Indeed, the most reactive is cyclization with the protonated pyrrole, where the activation barrier is estimated to be only 23.4 kcal mol^{-1}. The energy is higher than in the case of the separated diene and dienophiles, due to the energy necessary to orient them. Nevertheless, we expect that the intramolecular cycloaddition reaction will be facilitated with an entropy effect that is negligible for the intramolecular cycloaddition reactions.

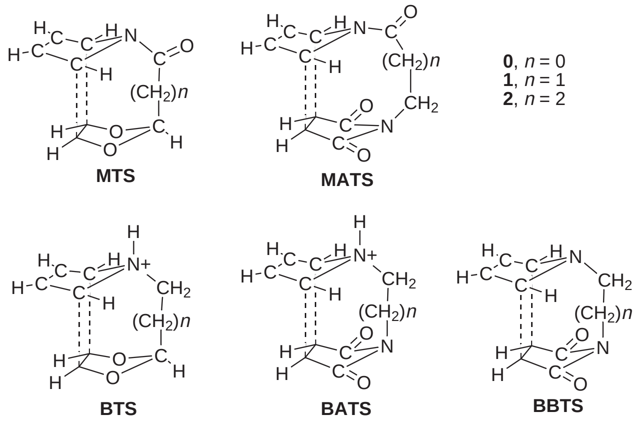

Fig. 3 Transition state structures for an intramolecular cycloaddition with pyrrole.

Table 7 The AM1 computed CC bond distances in the intramolecular cycloaddition with pyrrole derivatives

Structure	*n*	Reactant	Transition state	$r_{CC(1)}$/Å	$r_{CC(2)}$/Å
MTS	0	**MR0**	**MTS0**	2.094	2.094
	1	**MR1**	**MTS1**	2.077	2.118
	2	**MR2**	**MTS2**	2.066	2.138
MATS	0	**MAR0**	**MATS0**	2.056	2.056
	1	**MAR1**	**MATS1**	2.068	2.086
	2	**MAR2**	**MATS2**	2.090	2.092
BTS	0	**BR0**	**BTS0**	2.177	2.177
	1	**BR1**	**BTS1**	2.166	2.234
	2	**BR2**	**BTS2**	2.196	2.198
BATS	0	**BAR0**	**BATS0**	2.136	2.136
	1	**BAR1**	**BATS1**	2.134	2.181
	2	**BAR2**	**BATS2**	2.159	2.174
BBTS	0	**BBR0**	**BBTS0**	2.066	2.066
	1	**BBR1**	**BBTS1**	2.055	2.055
	2	**BBR2**	**BBTS2**	1.943	2.219
	3	**BBR3**	**BBTS3**	2.000	2.156

From the synthetic point of view, the utilization of **MAR0**, **MAR1** and **MAR2** as starting materials for the preparation of alkaloids is the most reasonable approach. Furthermore, the computed activation barrier for the cycloaddition reaction through transition state **MATS2** is only 35.5 kcal mol^{-1} (Table 9). Considering the fact that the molecule has amide bonds, and molecules with these functionalities are perfect candidates for the Lewis acid catalyzed cycloaddition, we believe that the activation barrier in the catalytic condition should be substantially lower. The preparation of the reactants is trivial, starting with an amino acid and maleic anhydride as outlined in Scheme 1. All reactions are straightforward and should afford intermediates and final products in quantitative yield.

One can also argue that the intramolecular cycloaddition reaction with reactants that have short methylene spaces should easily undergo an intermolecular rather than an intramolecular cycloaddition reaction. Indeed, that is true in the case of the reactant **MAR0**. The double cycloadduct transition state structure (Fig. 4) has a lower energy (~31 kcal mol^{-1}) than the corresponding intramolecular cycloadduct. Nevertheless, after hydrolysis of the cycloadduct, the same *exo* product as presented in Scheme 1 should be obtained.[30]

Conclusion

From the results presented in this paper, several conclusions can be made. First, pyrrole by itself is a very poor diene for the cycloaddition reaction due to its high aromaticity. The aroma-

Table 8 Bond order uniformity for the transition states (Fig. 3) with a six-membered ring being formed[a]

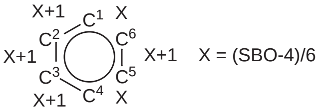

TS	BO_{12}	BO_{23}	BO_{34}	BO_{45}	BO_{56}	BO_{16}	X	SBOD
MTS2	1.206	1.628	1.192	0.460	1.314	0.439	0.373	0.815
MATS2	1.169	1.658	1.174	0.470	1.320	0.462	0.376	0.927
BTS2	1.402	1.418	1.402	0.349	1.360	0.359	0.382	0.154
BATS2	1.394	1.429	1.391	0.379	1.432	0.384	0.402	0.117
BBTS2	1.127	1.688	1.161	0.387	1.302	0.531	0.366	1.016

[a] BO_{nm} = bond order between the pyrrole ring atoms *n* and *m*; ABO = average ring bond order computed as sum of all rings bond orders divided by the number of atoms in the ring (five); SBOD = sum of ring's bond order deviation from an average bond order.

Table 9 Total energies (a.u.) for reactants and the transition state structures and activation barrier (kcal mol^{-1}) computed with B3LYP/6-31G(d)//AM1 theory model[a]

TS	E_R	E_{TS}	E_P	ΔE_I	ΔE_{II}
MTS0	−589.4062248	−589.3282223	−589.3883105	48.9	11.2
MTS1	−628.7276118	−628.6572975	−628.7119201	44.1	9.8
MTS2	−668.046859	−667.9826519	−668.0369624	40.3	6.2
MATS0	−721.0395197	−720.9467254	−720.9622930	58.2	48.5
MATS1	−760.3533037	−760.2887441	−760.3114048	40.5	26.3
MATS2	−799.670665	−799.6140644	−799.6451503	35.5	16.0
BTS0	−515.7110072	−515.6736869	−515.7608546	23.4	−31.3
BTS1	−555.0302272	−554.9841416	−555.0766733	28.9	−29.1
BTS2	−594.3463801	−594.2954979	−594.3853790	31.9	−24.5
BATS0	−608.0251442	−607.9338932	−607.9893424	57.3	22.5
BATS1	−647.3374926	−647.2469868	−647.3125978	56.8	15.6
BATS2	−686.6534285	−686.5772075	−686.6488811	47.8	2.9
BBTS0	−607.7031412	−607.6215211	−607.6367185	51.2	41.7
BBTS1	−647.0165489	−646.9365725	−646.9501405	50.2	41.7
BBTS2	−686.3288314	−686.2680749	−686.2781346	38.1	31.8
BBTS3	−725.6427353	−725.5816141	−725.5971665	38.4	28.6

[a] E_R = total energy for the reactant; E_{TS} = total energy for the transition state; E_P = total energy for the product; ΔE_I = activation barrier (kcal mol^{-1}); ΔE_{II} = heat of the reaction (kcal mol^{-1}).

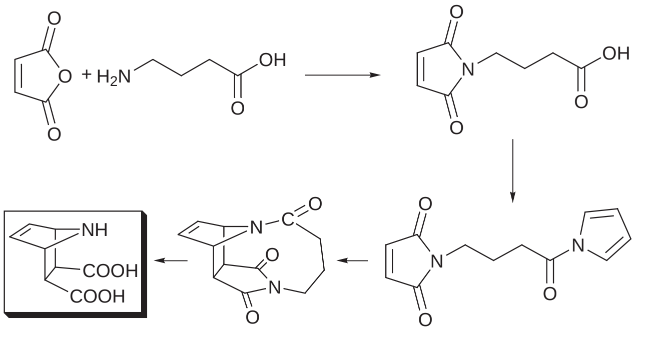

Scheme 1 Proposed synthetic path for preparation of an *exo* pyrrole cycloadduct based on our calculations.

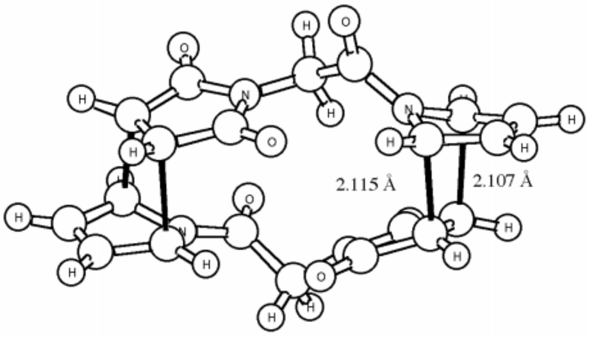

Fig. 4 Intermolecular double cycloadduct of **MAR0** computed with the AM1 semiempirical method.

ticity can be followed through bond order uniformity in the pyrrole ring where there is no clear localization of single and double bonds. The nitrogen lone pair of pyrrole is involved in molecular orbital overlap with two CC double bonds. The pyrrole derivatives that involve the nitrogen lone pair such as the pyrrolium cation destroy this effect, and double bonds are firmly located in the pyrrole ring making it a perfect diene for the Diels–Alder reaction. Other substituents such as *N*-formyl that will partially delocalize the nitrogen lone pair out of the pyrrole ring also increase its reactivity as a diene.

In all cycloaddition reactions, the *endo* cycloadduct is predicted to be the dominant, but not the only product. This is explained by secondary orbital interactions in the transition state, higher aromaticity of the *endo* transition state structure, and inertia factors through frontier molecular orbital energies as well as through activation reaction barriers. To enforce the formation of an *exo* cycloadduct that is a desirable intermediate for the preparation of alkaloids, the diene and the dienophile are combined *via* a methylene link within the same molecule. Intramolecular reactions with proper geometry have slightly higher activation barriers but should be experimentally feasible. In the case of short spaces, the intermolecular cycloaddition reaction is preferred, but the final reaction outcome is the same. Therefore these synthetic schemes are suggested as ones that should be experimentally feasible and result in the preparation of the *exo* isomer only.

Acknowledgements

The author is thankful to the referees for very constructive comments. This work is supported by the Louisiana Educational Quality Support Fund (LEQSF-RD-A-30) and by National Science Foundation grant no. CHE-9512155.

References

1 W. Carruthers, in *Cycloaddition Reactions in Organic Synthesis; Tetrahedron Organic Chemistry Series*, Vol. 8, Pergamon Press, Elmsford, NY, 1990; F. Pontén and G. Magnusson, *J. Org. Chem.*, 1997, **67**, 7978; B.-C. Hing, S.-S. Sun and Y.-C. Tsai, *J. Org. Chem.*, 1997, **62**, 7717.

2 O. Diels and K. Alder, *Justus Liebigs Ann. Chem.*, 1928, **460**, 98; J. A. Norton, *Chem. Rev.*, 1942, **31**, 319; M. C. Kloetzel, *Org. React.*, 1948, **5**, 136; L. W. Butz and A. W. Rytina, *Org. React.*, 1949, **5**, 136; J. Sauer, *Angew. Chem.*, *Int. Ed. Engl.*, 1966, **5**, 211; H. Kault and K. King, *Chem. Rev.*, 1968, **68**, 415; S. B. Needleman and M. C. Chang Kuo, *Chem. Rev.*, 1962, **62**, 405; J. G. Martin and R. K. Hill, *Chem. Rev.*, 1961, **61**, 537; L. C. Dias, *J. Braz. Chem. Soc.*, 1997, **8**, 289; N. K. Houk, J. González and Y. Li, *Acc. Chem. Res.*, 1995, **28**, 81; K. N. Houk, Y. Li and J. D. Evanseck, *Angew. Chem.*, *Int. Ed. Engl.*, 1992, **31**, 682; B. A. Horn, J. L. Herek and A. H. Zewail, *J. Am. Chem. Soc.*, 1996, **118**, 8755.

3 For instance see: D. L. Boger and S. N. Weinreb, *Hetero Diels-Alder Methodology in Organic Synthesis*, Academic Press, New York, NY, 1987; D. L. Boger, *Chem. Rev.*, 1986, **86**, 781; R. R. Schmidt, *Acc. Chem. Res.*, 1986, **19**, 250.

4 B. S. Jursic, *J. Heterocycl. Chem.*, 1995, **32**, 1445; B. S. Jursic, *J. Heterocycl. Chem.*, 1995, **32**, 483.

5 Y. Li, T. Thiemann, T. Sawada, S. Mataka and M. Tashiro, *J. Org. Chem.*, 1997, **62**, 7926 and references therein.

6 B. S. Jursic and Z. Zdravkovski, *J. Mol. Struct. (THEOCHEM)*, 1995, **332**, 39; B. S. Jursic, *J. Mol. Struct. (THEOCHEM)*, 1996, **365**, 55; B. S. Jursic, *J. Org. Chem.*, submitted.

7 Z. Chen and M. L. Trudell, *Chem. Rev.*, 1996, **86**, 1179 and references therein.

8 M. J. S. Dewar, E. G. Zoebisch, E. F. Healy and J. J. P. Stewart, *J. Am. Chem. Soc.*, 1985, **107**, 3902.

9 MOPAC, version 6.0. Quantum Chemistry Program Exchange (QCPE), Program Number 455, Bloomington, IN, 1984.

10 D. R. Armstrong, P. G. Perkins and J. J. P. Stewart, *J. Chem. Soc.*, *Dalton Trans.*, 1973, 838.

11 A. D. Becke, *J. Chem. Phys.*, 1993, **98**, 5648; C. Lee, W. Yang and R. G. Parr, *Phys. Rev. B*, 1988, **37**, 785.

12 M. M. Francl, W. J. Pietro, W. J. Hehre, J. S. Binkley, M. S. Gordon, D. J. DeFrees and J. A. Pople, *J. Chem. Phys.*, 1982, **77**, 3654.

13 GAUSSIAN94, Revision B.3, M. J. Frisch, G. W. Trucks, H. B. Schlegel, P. M. W. Gill, B. G. Johnson, M. A. Robb, J. R. Cheeseman, T. Keith, G. A. Petersson, J. A. Montgomery, K. Raghavachari, M. A. Al-Laham, V. G. Zakrzewski, J. V. Ortiz, J. B. Foresman, C. Y. Peng, P. Y. Ayala, W. Chen, M. W. Wong, J. L. Andres, E. S. Replogle, R. Gomperts, R. L. Martin, D. J. Fox, J. S. Binkley, D. J. Defrees, J. Baker, J. P. Stewart, M. Head-Gordon, C. Gonzalez and J. A. Pople, Gaussian, Inc., Pittsburgh, PA, 1995.

14 For a general definition and examples of aromaticity see: P. J. Garrat, *Aromaticity*, Wiley, New York, 1986; D. Lewis and D. Peters, *Facts and Theory of Aromaticity*, Macmillan, London, 1975; V. I. Minkin, M. N. Glukhovtsev and B. Y. Simkin, *Aromaticity and Antiaromaticity: Electronic and Structural Aspects*, Wiley, New York, 1994; J. P. Snyder, *Nonbenzenoid Aromatics*, Academic Press, New York, 1969, vol. 1, ch. 1; M. J. Glukhovtsev, *Chem. Educ.*, 1997, **74**, 132 and references therein.

15 B. S. Jursic, *J. Heterocycl. Chem.*, 1997, **34**, 1387; B. S. Jursic, *J. Heterocycl. Chem.*, 1996, **33**, 1079.

16 B. S. Jursic, 'Cycloaddition Reactions Involving Heterocyclic Compounds as Synthons in the Preparation of Valuable Organic Compounds. An Effective Combination of a Computational Study and Synthetic Applications of Heterocycle Transformations', in *Computational Organic Chemistry*, ed. C. Párkányi, Elsevier, Amsterdam, 1998.

17 One can always raise a question about the reliability of the AM1 computed bond orders. This question exists for all computational methods regardless of the used theory level. We have demonstrated that qualitative results obtained on the heterocycle bond order are identical regardless of whether they were computed with the AM1, *ab initio*, or density functional theory methods.[16]

18 M. G. Evans, *Trans. Faraday Soc.*, 1939, **35**, 824.

19 H. E. Zimmerman, *J. Am. Chem. Soc.*, 1966, **88**, 1566; H. E. Zimmerman, *Acc. Chem. Res.*, 1971, **4**, 272; H. E. Zimmerman, *Tetrahedron*, 1982, **38**, 753.

20 M. J. S. Dewar, *Tetrahedron Suppl.*, 1966, **8**, 75; M. J. S. Dewar, *Angew. Chem.*, *Int. Ed. Engl.*, 1971, **10**, 761.

21 K. Alder and G. Stein, *Angew. Chem.*, 1937, **50**, 510.

22 R. B. Woodward and R. Hoffmann, *The Conservation of Orbital Symmetry*, Verlag Chemie, Weinheim, 1971.

23 G. Lendvay, *J. Phys. Chem.*, 1994, **98**, 6098 and references therein.

24 B. S. Jursic, *Tetrahedron Lett.*, 1977, **38**, 1305.

25 B. S. Jursic, *J. Org. Chem.*, 1977, **62**, 3046; B. S. Jursic, *J. Mol. Struct.* (*THEOCHEM*), in the press.

26 K. Fukui, *Theory of Orientation and Stereochemistry*, Springer-Verlag, Berlin, 1975; K. N. Houk, *Acc. Chem. Res.*, 1975, **8**, 361; K. Fukui, *Angew. Chem.*, *Int. Ed. Engl.*, 1982, **21**, 801; I. Fleming, *Frontier Orbitals and Organic Chemistry Reactions*, Wiley, London, 1976, ch. 4.

27 B. S. Jursic, *J. Mol. Struct.* (*THEOCHEM*), in the press. In this paper, the position of the transition state, as well as the inertia principle were thoroughly discussed in comparison with relevant literature.

28 M. G. Jung and J. C. Rohloff, *J. Chem. Soc.*, *Chem. Commun.*, 1984, 630; E. Ciganek, *J. Org. Chem.*, 1980, **45**, 1512.

29 For instance see: B. S. Jursic, Computing Transition State Structures with Density Functional Theory Methods, in *Recent Developments and Applications of Modern Density Functional Theory*, ed. J. M. Seminario, Elsevier, Amsterdam, The Netherlands, 1996, p. 709.

30 Experimental results that were obtained on the basis of these computational studies will be published elsewhere.

Paper 8/03740J